Case Studies in Thermal Engineering 27 (2021) 101239

Contents lists available at ScienceDirect

Case Studies in Thermal Engineering

journal homepage: www.elsevier.com/locate/csite

On bioconvection and mass transpiration of micropolar nanofluid dynamics due to an extending surface in existence of thermal radiations

Danial Habib [a], Sohaib Abdal [b], Rifaqat Ali [c,***], Dumitru Baleanu [d,e,f,*], Imran Siddique [g,**]

[a] Department of Mathematics, Khwaja Fareed University of Engineering and Information Technology, Rahim Yar Khan, Pakistan
[b] School of Mathematics, Northwest University, Xi'an, China
[c] Department of Mathematics, College of Science and Arts, King Khalid University, Muhayil, 61413, Abha, Saudi Arabia
[d] Department of Mathematics, Cankaya University, 06530, Balgat, Ankara, Turkey
[e] Institute of Space Sciences, Magurele-Bucharest, Magurele-Bucharest, Romania
[f] Department of Medical Research, China Medical University Hospital, China Medical University, Taichung, Taiwan
[g] Department of Mathematics, University of Management and Technology, Lahore 54770, Pakistan

ARTICLE INFO

Keywords:
Non-linear geometry
Micropolar
Nanoparticles
Motile microorganism
Shooting technique

ABSTRACT

This study examines the magnetic effects of heat and mass transmission on the flow of micropolar fluid over a permeable stretching geometry with dilute homogeneous dispersion of nano-particles and gyrotactic microorganisms. A system of coupled highly non-linear PDEs is renovated into corresponding ODEs by using similarity functions. These transmuted equations are resolved for a solution with shooting technique accompanied with Runge-Kutta fourth order. The variations of intricate physical quantities such as temperature, micro-motion, concentration, velocity, and motile micro-organism profiles are evaluated under the influence of the emerging parameters. The velocity profile decreases down with upsurge values of magnetic parameter M while micro-rotation is strengthened and its value becomes higher directly with increments in M. The microorganisms profile depict the diminishing behavior with the growing value of bioconvection Lewis number. These results are useful for obtaining better solutions for heat transfer devices and micropolar fuel cells. Additionally, the impact of the parameter of Brownian motion, Rayleigh number, and the parameter of thermophoresis, Peclet number, and buoyancy ratio parameter were discussed numerically and graphically. Moreover, the numerical results were validated by comparing them with previously obtained exact solution for special cases and acceptable compatibility between the two results is achieved. The findings from this work can be utilized for efficient heat exchangers and thermal balance in micro-electronics.

* Corresponding author. Department of Mathematics, Cankaya University, 06530, Balgat, Ankara, Turkey.
** Corresponding author.
*** Corresponding author.
E-mail addresses: dumitru.baleanu@gmail.com (D. Baleanu), imransiddique@umt.edu.pk (I. Siddique).

https://doi.org/10.1016/j.csite.2021.101239
Received 7 June 2021; Received in revised form 3 July 2021; Accepted 9 July 2021
Available online 15 July 2021

1. Introduction

Nomenclature

Latin symbols

x, y	cartesian coordinates
ν	kinematic viscosity
N	microrotation vector
j	microinertia
T	temperature
T_w	convective fluid temperature
T_∞	ambient temperature
D_B	Brownian motion constant
D_T	thermophoretic constant
C	nano-particles concentration
C_w	concentration at the wall
C_∞	ambient concentration
A	motile density of microorganisms
A_W	density of motile micro-organism
A_∞	ambient motile microorganisms
b_1	chemotaxis constant
W_c	maximum cell swimming speed
Dm	diffusion coefficient of microorganisms
Nu_x	local Nusselt number
Re	local Reynolds number
V_o	parameter of transpiration injection/suction
Re	Reynolds number
K	material parameter
Pr	Prandtl number
Le	Lewis number
Lb	bio-convection Lewis number
Pe	bio-convection Peclet number
Rd	radiation parameter
Cf_x	skin friction
Sh_x	sherwood number
Nn_x	motile density number
q_n	motile microorganism flux
q_w	surface heat flux
q_m	surface mass flux
t_w	shear stress
Nb	Brownian motion parameter
Nt	thermophoresis parameter

Greek symbols

ρ	fluid density
α	electrical conductivity
γ	spin gradient
τ	ratio between heat capacities of fluid and nanoparticle
ψ	stream function
Ω	microorganism concentration difference

Research on generalized flows has drawn attention to the importance of micropolar fluids. Such contemplations are due to the fact that Newtonian fluids cannot adequately represent the functions of fluid flow in many commercial applications and organisms. The theory of internal motion and the local characteristics that emerged from the microstructure was presented by Eringen [1]. This theory characterizes synthetic substances such as lubricants, animal blood, polymers, paints, and colloidal solutions. The micropolar fluid model is used to indicate the presence of emulsions. In addition, the micropolar fluid model is extremely important in the stability of liquid crystals. Micropolar fluid extended into thermo-micropolar fluid also presented by Eringen [2]. The stiff particles in a slight volume element turn around the centroid of the volume segment in micropolar fluids. Results of MHD mixed convection flow for the

nonlinear heat with convective boundaries have been expressed by Waqas et al. [3]. Ali et al. [4] investigated the effect of magnetic properties of micropolar based nano-particles due to a magnetic dipole. Abdal et al. [5] worked on the effects of thermo-diffusion and multislips on MHD micropolar based nanofluids. Liaqat et al. [6] studied magnetic dipole in micropolar fluid flow by using finite element method. Ali [7] studied advancements in PV cooling and efficiency enhancement. Ejaz et al. [8] increased the thermal energy in technologies. Akram et al. [9] studied the turbulence effects between parallel triangular tube array. Khader et al. [10] described the multiple features of MHD micropolar fluid along heat source/sink over sheet but Tlili et al. [11] designated the MHD micropolar nanofluid with bioconvection and motile microorganisms. The discovery occurs when Huang et al. [12] presents the global dynamics of a three-dimensional compressible micropolar fluid with vacuum and large oscillations.

From an industrial perspective, heat transfer efficiency is the greatest need of today. Ordinary cooling agents are not able to meet the needs of future industries. Nanotechnology requires efficient technology. This phenomenon involves nano-entities, 100 nm in size, they are found in ethylene, water, oil, or glycol. The nanoparticles trapped in nanomaterials usually consist of metals, oxides, carbon graphite, nitrides, carbides, and nanotubes. After that several methods have since been discovered that are responsible for improving the thermal exposure of nanofluids. These methods include nanoparticles, thermal diffusion, Brownian motion, thermophoresis, etc. According to experimental research on nanoparticles, the participation of nano-size particles in base fluids involved thermophysical properties such as the thermal conductivity of liquids presented by Choi and Eastman [13]. Buongiorno [14] examined that the thermal presentation of base liquid is improved because of thermophoresis factors and Brownian motion. Ahmad et al. [15] address the unstable, three-dimensional nanofluid flow due to the behavior of thermophoresis and Brownian motion. The flow of the Buongiorno model over a conductive, significantly extended network is defined by Alblawi et al. [16]. Hayat et al. [17] analyze the three-dimensional magnetohydrodynamic flow of nanofluids through a non-linear biocompatible surface with control of nano-materials internally and externally. Sohaib et al. [18] find the uniqueness and existence of MHD Casson nanofluid. Ali et al. [19] numerically discussed the effects of Stefan blowing on thermal radiation and Cattaneo–Christov characteristics for nanofluid flow. Hussain et al. [20] discussed buoyancy effect on heat transfer of a nanofluid flow passing over a plate. Bagh et al. [21] discussed variable viscosity effects on time dependent MHD nanofluid flow over a stretching surface. Boundary layer flow and heat transfer effects of nanofluid in the presence of a heat source were discussed by Abbas et al. [22]. Time dependent MHD Casson nanofluid flow with radiation and heat source was discussed by Liaqat et al. [23]. Similar work were done by Refs. [24–28].

Bio-convection is a process in which small size microbe float in the upper part of a fluid, causing irregular formation and instability. Due to the rapid swimming, these gyrotactic micro-organisms such as algae are likely to accumulate in the upper layer of fluid which causes an unstable peak resulting in heavy density stabilization. The two effects of Brownian motion and thermophoresis effect generate the motion of nanoparticles. The motion of motile micro-organisms is not affected by nanoparticle motion So that the joint interface of bio convection and nanofluids turn out to be important for micro-fluidic appliances. Nanofluids and bio-convection are therefore relatively interesting for recent micro-fluidic appliances. The two effects of browning motion and thermophoresis effect are the movement of nanoparticles. The movement of micro-organisms is not affected by the motion of nanoparticles so that the combined interface of bioconvection and nanofluids emerges for microfluid appliances. Kuznetsov and Avramenko [29] looked at bioconvection during the suspension of gyrotactic micro-organisms. Bees et al. [30] discussed the word bioconvection which describes hydrodynamic instability and patterns in life-swimming body fluids. Khan et al. [31] explore the scientific foundation of neutralizing nanoparticles over a given base fluid, this task can be performed and subsequent nanofluids increase the heat capacity of the base fluids. Khan et al. [32] examine the significance of the movement of nanofluid bioconvection across the supposedly oscillatory stretched sheet. Bio-convection plays its role for various scientific, manufacturing, economic, and social materials is intended to investigate motile mi-croorganisms, such as their variations in swimming.

The phenomenon of boundary laminar flow on a stretch surface with constant heat transfer is important in terms of its mechanical as well as design applications. Such stream flow usually includes wire drawing, extrusion of soft leaves, glass fiber creation, hot systematic, chilling of metal salver in cooling dip, and others. Researchers commonly measure the flow at the stretching surface, yet modern and advanced measures have conditions where the stretching surface is not normally linear, mainly driven by a nine-liner pulling sheet. Villa stream plays an important role in polymer emissions. The watercourse issues about its collection and shape have more ranked to polymer extrusions by a stretching surface. Vajravelu [33] examined the belongings of heat transfer about sticky fluid flow which is prompted by a nonlinear surface. Cortell [34] accomplished a mathematical report to discover the nonlinear gluey fluid flow over a stretching surface. After that, the work about the measurement of heat transfer is specified the two instances of the recommended external temperature. The boundary layer flow over a porous nonlinear extending sheet is also noticed by Mukho-padhyay [35]. Sajjad et al. [36] worked on the enhancement of highly melted liquid. Parsa et al. [37] discussed the effects of *Ag*, *Au*, *TiO*2 metallic/metal oxide nanoparticles in double-slope solar stills. Khechekhouche et al. [38] discussed energy analysis, and Opti-mizations of Collector Cover. Gireesha et al. [39] demonstrated the effects of nonlinear MHD Jaffrey nanofluid updraft radiation over a nonlinear permeable sheet. Another extension of activation energy and convective heat/mass transfer effects on third-grade nanofluid over a nonlinearly stretching surface is deliberate by Hayat et al. [40].

The above-mentioned studies explored nanofluid dynamics with simple base-fluids. The varied intention of this work pertains to micropolar-based nanofluids with implications of bio-convections and thermal radiations. The manipulation of the related formulation is difficult due to the inherent nonlinearity involved. Apposite similarity variables transmute the leading equations into ordinary differential form. Then numerical solutions are obtained via the Runge-Kutta method. The Matlab based computational endeavor resolved the numerical solution of the coupled governing differential formulation. Here the results may find applications in the heat exchanger and thermal efficiency of micro-systems.

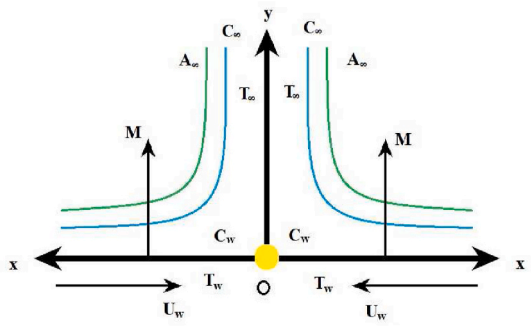

Fig. 1. Problem description.

2. Physical model and mathematical formulation

The transportation of micropolar nanofluid due to non-linear permeable stretching surface is taken into account. The assumptions of the current formulation include a steady flow of an electrically conducting and incompressible fluid issuing from a slit at the origin as shown in Fig. 1 The geometry is assumed to be horizontal and coincides with the plane $y = 0$. A dilute dispersion of nanoparticles and self-propelled micro-organisms is an inhomogeneous phase with the fluid. A magnetic field of strength B_0 acts vertically. To spread it, on $x - axis$ two equal and opposite forces were applied to the sheet. Also $(U_1, 0)$ is the applied stretching velocity of the sheet.

Furthermore, magnetic Reynolds number is considered extremely small with the purpose of excluding the magnetic field of stimulation. With these principles, the under discussed administrative equations are

$$U_1 = U_0\left(\frac{x}{p}\right)^m$$

$$B_0 = \left(0, B_0\left(\frac{x}{p}\right)^{\frac{m-1}{2}}\right)$$

The velocity of mass transpiration is

$$W_1 = W_0\left(\frac{x}{p}\right)^m$$

Where W_0 and p are the specified velocity and distance. $m > -1$ is the stretching index. The permeability of medium is

$$V_1 = -V_0\sqrt{\frac{m+1}{2}}\left(\frac{x}{p}\right)^{\frac{m-1}{2}}$$

For convention we use $(V_1 > 0, V_1 < 0)$ suction and injection of the fluid at $y = 0$. The widening of the sheet tempts a velocity field in liquids $(u(x, y), v(x, y))$ which is satisfied the continuity. $N = -n_0\left(\frac{\partial u}{\partial y}\right)$, the disorder for micropolar particles [3]. The following is an expression of the governing problems in approaching the boundary layer represents the equations of continuity, momentum, micropolar, energy, concentration and concentration of micro-organisms [3,41]:

$$\frac{\partial u}{\partial x} + \frac{\partial v}{\partial y} = 0, \tag{1}$$

$$\left(\frac{\mu + k_1}{\rho}\right)\frac{\partial^2 u}{\partial y^2} + \frac{k_1}{\rho}\frac{\partial N}{\partial y} - \frac{\sigma B_0^2 u}{\rho} = u\frac{\partial u}{\partial x} + v\frac{\partial u}{\partial y}, \tag{2}$$

$$\frac{k_1}{\rho j}\left(2N + \frac{\partial u}{\partial y}\right) + u\frac{\partial N}{\partial x} + v\frac{\partial N}{\partial y} = \frac{\gamma}{\rho j}\frac{\partial^2 N}{\partial y^2}, \tag{3}$$

$$\frac{1}{(\rho C)_f}\left(\frac{\partial q_r}{\partial y}\right) + u\frac{\partial T}{\partial x} + v\frac{\partial T}{\partial y} = \alpha\frac{\partial^2 T}{\partial y^2} + \tau\left[D_B\frac{\partial C}{\partial y}\frac{\partial T}{\partial y} + \frac{D_T}{T_\infty}\left(\frac{\partial T}{\partial y}\right)^2\right], \tag{4}$$

$$u\frac{\partial C}{\partial x} + v\frac{\partial C}{\partial y} = D_B\frac{\partial}{\partial y}\frac{\partial C}{\partial y} + \frac{D_T}{T_\infty}\frac{\partial}{\partial y}\frac{\partial T}{\partial y}, \tag{5}$$

$$u\frac{\partial A}{\partial x}+v\frac{\partial A}{\partial y}=-b_1W_c\frac{\partial}{\partial y}\left(\frac{A}{\Delta C}\frac{\partial C}{\partial y}\right)+D_m\frac{\partial}{\partial y}\frac{\partial A}{\partial y}. \tag{6}$$

Here ρ represents fluid density, σ is electrical conductivity, ν is kinematic viscosity, γ is spin gradient, N is micro-rotation vector, j is microinertia, τ represents the ratio between heat capacities of fluid and nanoparticle, T is temperature, T_w is convective fluid temperature, T_∞ is ambient temperature, D_B stands for Brownian motion constant, D_T represents thermophoretic constant, C is nanoparticles concentration, C_w is the concentration at the wall, C_∞ is ambient concentration, A is motile density of microorganisms, A_w density of motile micro-organism, A_∞ ambient motile microorganisms, b_1 is chemotaxis constant, Wc is the maximum cell swimming speed, ΔC, D_m is the diffusion coefficient of microorganisms.

The supportive boundaries are:

$$\left.\begin{aligned} u=W_1, v=U_1, N=-n_0\frac{\partial u}{\partial y}, T-T_w=0, C-C_w=0, A-A_w=0,\ as\ y=0,\\ u\to 0,\ N\to 0,\ T\to T_\infty,\ C\to C_\infty,\ A\to A_\infty\ as\ y\to\infty. \end{aligned}\right\} \tag{7}$$

Using the similarity variables [42]:

$$\left.\begin{aligned} \xi &= \sqrt{\frac{Re(m+1)}{2}}\left(\frac{x}{P}\right)^{\frac{m-1}{2}}\frac{y}{P},\ u=U_1f'(\xi),\ v=\frac{V_1}{V_0}\left[f(\xi)+\frac{m-1}{m+1}\xi f'(\xi)\right],\\ N&=\left(\frac{x}{P}\right)^m\sqrt{\frac{Re(m+1)}{2\nu}},\\ \theta(\xi)&=\frac{T-T_\infty}{T_w-T_\infty},\ \varphi(\xi)=\frac{C-C_\infty}{C_w-C_\infty},\ \chi(\xi)=\frac{A-A_\infty}{A_w-A_\infty} \end{aligned}\right\} \tag{8}$$

The radiative heat flux q_r [23] is given as $q_r=\frac{-4\sigma_s}{3k^*}\frac{\partial T^4}{\partial y}$, where k^* stands for absorption constant and σ_s is Stefan-Boltsmann constant. By using Taylor series expansion for T^4 about T_∞, to yield

$$T^4\approx 4T_\infty^3T-3T_\infty^4$$

Then

$$q_r=\frac{16\sigma_sT_\infty^3}{3k^*k}$$

The stream function is $\psi=\nu\sqrt{\frac{2\mathrm{Re}}{m+1}}\left(\frac{x}{P}\right)^{\frac{m+1}{2}}f(\eta)$, $V_0=\frac{1}{\sqrt{Re}}\left(\frac{V_1P}{\nu}\right)$ Is the parameter of transpiration injection/suction and $\mathrm{Re}=\frac{W_0P}{\nu}$ is Reynolds number. Eq. (1) is satisfied and Eqs. (2)–(6) respectively become:

$$f'''+Kf''''-f'^2\frac{2m}{m+1}+ff''+Kg'-f'\frac{2M}{m+1}=0, \tag{9}$$

$$\left(1+\frac{K}{2}\right)g''+fg'-\frac{3m-1}{m+1}f'g-\frac{2K}{m+1}(2g+f'')=0, \tag{10}$$

$$(1+Rd)\theta''+Prf\theta'+Pr^*Nb\theta'\varphi'+Pr^*Nt\theta'^2=0, \tag{11}$$

$$\varphi''+Le^*Pr(f\varphi')+\left(\frac{Nt}{Nb}\right)\theta''=0, \tag{12}$$

$$\chi''-Lb(f\chi')-Pe[\varphi''(\chi+\Omega)+\chi'\varphi']=0. \tag{13}$$

$$\left.\begin{aligned} f(0)=S,\ f'(0)=1,\ g(0)=-n_0f''(0),\ \theta(0)=1,\ \varphi(0)=1,\ \xi(0)=1,\ at\ \xi=0,\\ f'(\infty)\to 0,\ N\to 0,\ \theta(\infty)\to 0, \varphi(\infty)\to 0, \chi(\infty)\to 0,\ as\ \xi\to\infty. \end{aligned}\right\} \tag{14}$$

Where $K=\frac{k_1}{\mu}$, $Pr=\frac{\nu}{\alpha}$, $Le=\frac{\alpha}{D_B}$, $Lb=\frac{\alpha}{D_m}$, $Pe=\frac{b_1Wc}{D_m}$, $\Omega=\frac{A_\infty}{A_w-A_\infty}$, $Nb=\frac{\tau D_B(C_w-C_\infty)}{\nu}$, $Nt=\frac{\tau D_T(T_w-T_\infty)}{\nu T_\infty}$, $Rd=\frac{16\sigma^*T_\infty^3}{3k^*K}$.

The physical quantities are stated as ([3,43]):Cf_x (skin friction coefficient), Nu_x (local Nusselt number), Sh_x (local Sherwood number) and Nn_x (local density of microorganism) are given below:

$$Cf_x=\frac{2\tau_w}{\rho U^2w}, Nu_x=\frac{xq_w}{k_1(T_w-T_\infty)}, Sh_x=\frac{xq_m}{D_B(C_w-C_\infty)}, Nn_x=\frac{xq_n}{D_m(N_w-N_\infty)},$$

Table 1
The comparative outputs for skin friction $-f''(0)$.

S	Singh et al. [42]	Present Results
−1.0	0.8639	0.8632
0.0	1.2349	1.2349
1.0	1.8104	1.8101
2.0	2.5619	2.5614

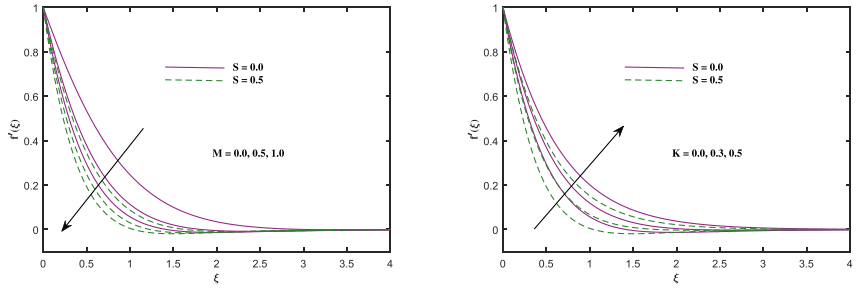

Fig. 2. Plot for velocity profile $f'(\xi)$ with varying values of M and K.

here q_n, q_w, q_m and τ_w denotes motile microorganism flux, surface heat flux, surface mass flux and shear stress are given by (at $y = 0$).

$$\tau_w = (\mu + K)\frac{\partial u}{\partial y} + KN,\ q_w = -K_1\frac{\partial T}{\partial y},\ q_m = -D_B\frac{\partial C}{\partial y},\ q_n = -D_m\frac{\partial N}{\partial y}.$$

On solving these quantities with the help of given similarity transformation, we obtain:

$$C_f = \frac{1}{(Re_x)^{1/2}}\sqrt{\frac{n+1}{2}}(1 + (1 - m_0)K)f''(0),\ Nu_x = -\frac{1}{(Re_x)^{-1/2}}\sqrt{\frac{n+1}{2}}\theta'(0),\ Sh_x = -\frac{1}{(Re_x)^{-1/2}}\sqrt{\frac{n+1}{2}}\varphi'(0),\ Nn_x = -\frac{1}{(Re_x)^{-1/2}}\sqrt{\frac{n+1}{2}}\chi'(0),$$

where, $(Re_x) = \frac{xU_w}{\nu}$ is the local Reynolds number.

3. Solution procedure

In this segment, numerical results for dimensionless nonlinearly coupled ordinary differential equations Eq. (9) to Eq. (13) with boundary conditions Eq. (14) are integrated by Runge-Kutta method of order four along with shooting technique. To execute this numerical method, the differential equations Eq. (9)–(13) are transformed into a first-order system with implementation of some new variable expressed as below.

$$s_1' = s_2$$
$$s_2' = s_3$$
$$(1 + K)s_3' = \frac{2m}{m+1}s_2^2 - s_1s_3 - Ks_5 + \frac{2M}{m+1}s_2$$
$$s_4' = s_5$$
$$(1 + K/2)s_5' = \frac{3m-1}{m+1}s_2s_4 - s_1s_5 - \frac{2K}{m+1}(2s_4 + s_3)$$
$$s_6' = s_7$$
$$(1 + Rd)s_7' = -Prs_1s_7 - PrNbs_7s_9 - PrNts_7^2$$
$$s_8' = s_9$$
$$s_9' = -LePrs_1s_9 - \frac{Nt}{Nb}ds_7$$
$$s_{10}' = s_{11}$$
$$s_{11}' = Lbs_1s_{11} + Pe[s_9s_{11} + (\Omega + s_{10})ds_9]$$

along with the boundary conditions:

$$s_1 = S,\ s_2 = 1,\ s_3 = g,\ s_4 = -n_0s_3,\ s_5 = h,\ s_6 = 1,\ s_7 = i,\ s_8 = 1,\ s_9 = j,\ s_{10} = 1,\ s_{11} = k,\ \text{at}\ \xi = 0.$$
$$s_2 \to 0,\ s_4 \to 0,\ s_6 \to 0,\ s_8 \to 0,\ s_{10} \to 0\ as\ \xi \to \infty.$$

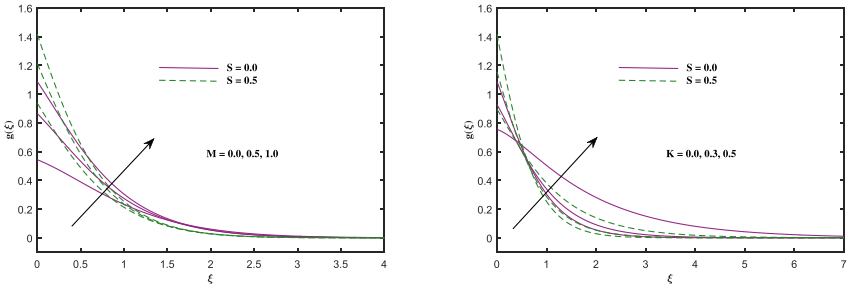

Fig. 3. Plot for $g(\xi)$ with varying values of M and K.

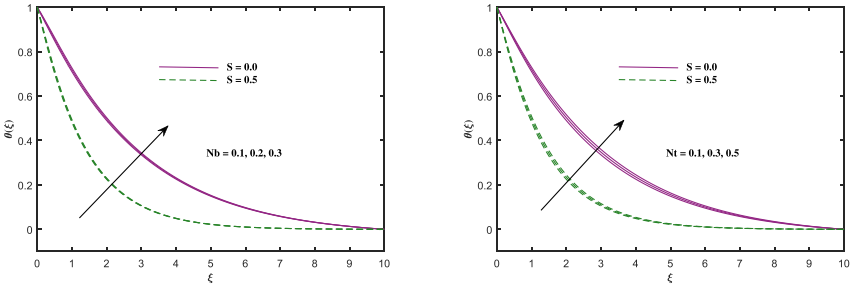

Fig. 4. Plot for temperature profile $\theta(\xi)$ with varying values of Nb and Nt.

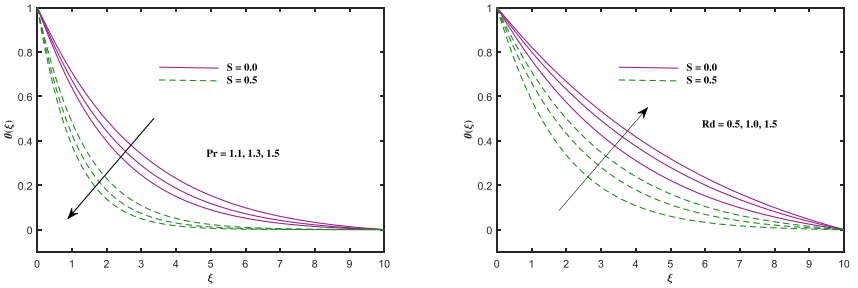

Fig. 5. Plot for temperature profile $\theta(\xi)$ with varying values of Pr and Rd.

The unknown initial conditions s_3, s_5, s_7, s_9, s_{11} are assigned arbitrary values to start the computational procedure. These values are finalized when the solution satisfies the boundary conditions.

4. Results and discussion

The numerical scheme as coded in the above segment for the approximate solution of the controlling equations to provide facility for physical insight. The behavior of velocity, temperature, nanoparticle volume fraction, micro-motion and micro-organisms density function is scrutinized when the influential parameters are varied in appropriate ranges. The current numeric results are validated when compared with the previous studies as limiting cases (see Table 1).

The pictorial descriptions of velocity, concentration, and thermal distributions are displayed in Figs. 2 to 7 for two cases of mass transpiration ($S = 0$–0.5). The notable influences of the sundry parameters are observed in the ranges $0.0 \leq M \leq 1.0$, $0.0 \leq K \leq 0.5$, $0.1 \leq Nb \leq 0.3$, $0.1 \leq Nt \leq 0.5$, $1.1 \leq Pr \leq 1.5$, $0.5 \leq Pr \leq 1.5$, $4.0 \leq Le \leq 6.0$, $0.4 \leq Pe \leq 1.2$, $0.4 \leq Lb \leq 1.2$ and $0.0 \leq \Omega \leq 0.2$. Fig. 2 demonstrates reducing behavior of velocity against the parameter M and reciprocal behavior with micropolar parameter K. Incremental input of M means the larger resistive force known as Lorentz force which causes inhibit the flow. Moreover, the greater value of $K = (\frac{k}{\nu})$ lesser dynamic viscosity, and hence the flow become faster. Also, the velocity distribution recedes with non-zero mass transpiration ($S = 0.5$). Fig. 3 presents plots of micro-rotation $g(\xi)$ for variant values of M and K. It is noticed that micro-rotation is strengthened and its value becomes higher directly with increments in M. However the micro-rotation twists when $K = (\frac{k}{\nu})$ takes higher inputs, it increases near the boundary but recedes away from the boundary ($S = 0.5$). Fig. 4 is drawn to show the increasing behavior of

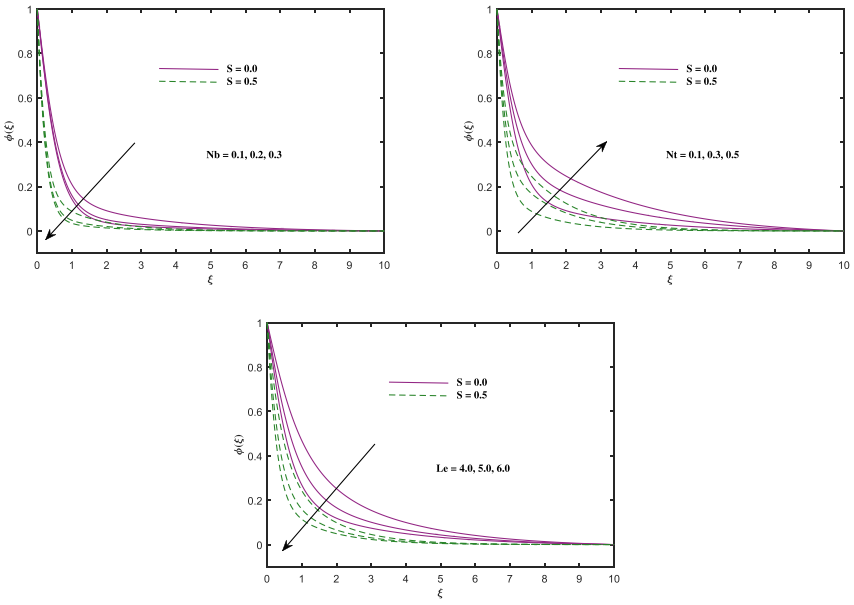

Fig. 6. Plot for concentration profile $\varphi(\xi)$ with varying values of *Nb*, *Nt* and *Le*.

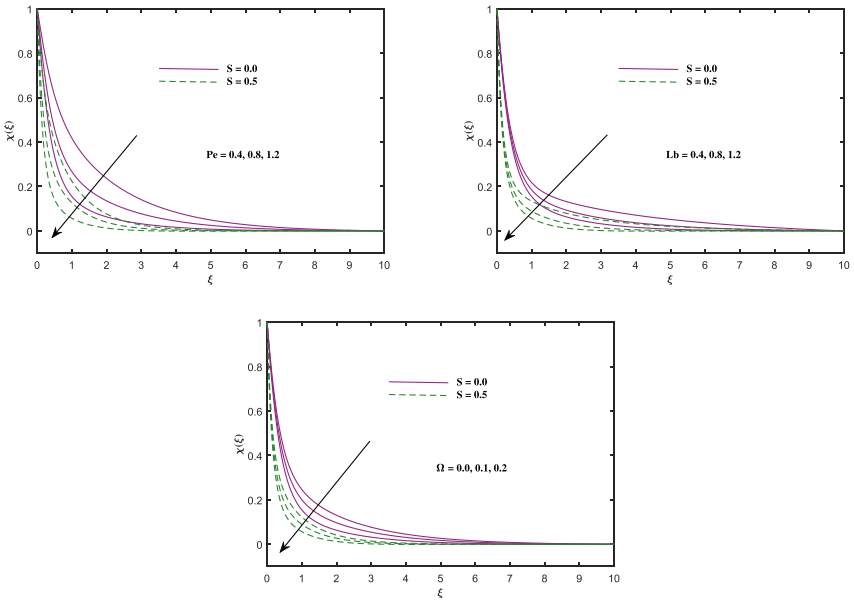

Fig. 7. Plot for $\chi(\xi)$ with varying values of *Pe*, *Lb* and Ω.

nanofluid temperature with rising inputs of *Nb* and *Nt*. It is also seen that the fluid temperature reduces significantly in the case of suction ($S = 0.5$). Physically, thermophoretic force is produced by temperature gradient and it produces actual wild flow from the stretching sheet. Thus, the fluid gets fierier and farther away from the surface and as a result, as the thermophoresis parameter *Nt* increases, the thickness of the thermal boundary layer increases and the temperature gradient on the surface decreases as *Nt* and *Nb* both increases. Fig. 5 is sketched to exhibits the averring behavior of temperature in the phase of *Pr* and *Rd*. The fluid temperature reduces vividly against higher values of *Pr*. It because the larger *Pr* means lesser diffusivity. In addition, the higher radiation parameter rises the fluid temperature because of exceeding radiative thermal distribution. Fig. 6 display the curves of nano volume fraction $\varphi(\xi)$ for variant values of *Nb*, *Nt* and *Le*. The concentration goes down against the larger inputs of *Nb*, and *Le* while it enhances directly with *Nt*. Physically, Brownian motion is the irregular movement of the digestive tract elements, which causes a substance to become obstructed, causing them to collide with moving particles in the fluid. This pattern of random motion typically transforms random

Table 2
Results for $-f''(0)$.

M	K	n_0	S	$m=-0.5$	$m=0$	$m=0.5$
0.5	0.5	0.1	0.5	1.4126	1.5065	1.6673
1.0				1.7523	1.8280	1.9476
1.5				2.0426	2.0974	2.1793
1.0	0.1			1.1651	1.1435	1.1207
	0.3			1.4917	1.4781	1.4613
	0.5			1.7523	1.8280	1.9476
	0.5	0.1		1.7523	1.8280	1.9476
		0.2		1.8955	1.9777	2.1072
		0.3		2.0385	2.1271	2.2666
		0.1	0.1	1.5102	1.5370	1.5765
			0.3	1.6275	1.6775	1.7539
			0.5	1.7523	1.8280	1.9476

Table 3
Results for $-\theta'(0)$.

Pr	Rd	Nb	Nt	$-\theta'(0)$
1.1	0.1	0.1	0.1	0.3576
1.3				0.4095
1.5				0.4580
1.1	0.1			0.3576
	0.5			0.2745
	1.0			0.2146
	0.1	0.1		0.3576
		0.2		0.3279
		0.3		0.3005
		0.1	0.1	0.3576
			0.2	0.3426
			0.3	0.3285

Table 4
Results for $-\varphi'(0)$.

Nt	Nb	Le	$-\varphi'(0)$
0.1	0.1	6.0	2.0017
0.2			1.7336
0.3			1.4884
0.1	0.1		2.0017
	0.2		2.1618
	0.3		2.2144
	0.1	2.0	0.5185
		4.0	1.2897
		6.0	2.0017

Table 5
Results for $-\xi'(0)$.

Lb	Pe	Ω	$-\chi'(0)$
0.4	1.2	0.2	3.0375
0.8			3.1881
1.2			3.3366
1.2	0.4		1.4599
	0.8		2.3959
	1.2		3.3366
	1.2	0.1	3.1034
		0.2	3.3366
		0.3	3.5699

disturbance in the particle position in the fluid subdomain with the transfer to another subdomain. With each transfer, the new closed system is further disrupted. This pattern describes a fluid in thermal equilibrium. Then thermophoresis phenomena, small particles of fluid are drawn back from the hot to cold area. Then, nanofluid particles recede from the surface, which heats up, resulting in an increase in temperature, thermal boundary layer, and nanoparticle volume fraction profiles. The distribution of motile micro-

organisms for different values of *Pr*, *Lb*, and Ω is plotted in Fig. 7. A view of these figures indicates the function $\chi(\xi)$ reduces significantly against increments of *Pe*, *Lb* and Ω. Moreover, the micro-organisms distribution function $\chi(\xi)$ reduces with mass transpiration ($S = 0.5$). Physically the Peclet number is a measure of the direction and movement of microorganisms. Therefore, the high values of the Peclet number indicate the maximum directional movement of swimming microorganisms, which depresses the field of moving microorganisms. The diffusivity of microorganisms is reduced to large estimates of *Lb*, which ultimately reduces the dynamic density of the fluid. This behavior is linked to the weak differentiation of microorganisms. Table 2 presents the upsurge in skin friction factor for increasing variation of parameters *M*, *K*, n_0 and *S* for all the cases of m ($m < 0$, $m = 0$, $m > 0$). Table 3 exhibits the enumeration of Nusselt number $-\theta'(0)$ which increase directly with *Pr* but recedes against *Rd*, *Nb*, and *Nt*. The Sherwood number $-\varphi'(0)$ notices that decline effects against the parameter *Nt* but it progresses directly *Nb* and *Le* as shown in Table 4. Table 5 indicates the rising magnitude of microorganism density $-\chi'(0)$ with increments in *Lb*, *Pe*, and Ω.

5. Conclusions

Mass transpiration and thermal radiation effects on micropolar-based nanofluid transportation due to a permeable and non-linear stretching sheets are studied in the presence of magnetic field and bio-convection. Some notable findings reveal briefly the impacts of leading parameters as described below:

- It is noticed that velocity decreases with the boosting values of *M* while upsurges with the higher inputs of *K*.
- Micro-rotation becomes higher directly with the rising values of *M* and *K*, However, the micro-rotation curve twisted behavior in the boundary regime.
- With the increasing values of *Rd*, *Nb* and *Nt*, temperature reduces rapidly but temperature goes down with the rising values of *Pr*.
- Concentration profile decreases for *Nb* and *Le* but rises for *Nt*.
- With the incremented values of *Pe*, *Lb*, and Ω, the motile density profile shows decreasing behavior.
- Skin friction factor directly upsurge with the rising values of *M*, n_0, *K*, and *S* for all three cases as discussed above.
- Nusselt number shows the decreasing pattern for *Rd*, *Nb*, and *Nt* but increases with *Pr*.
- Sherwood number uplifted for *Nb* and *Le* but recedes for *Nt*.
- Magnitude of micro-organism density number rises directly with *Lb*, Ω, and *Pe*.

CRediT authorship contribution statement

Danial Habib: Writing – original draft, Investigation. **Sohaib Abdal:** Conceptualization, Software. **Rifaqat Ali:** Methodology, Visualization, Validation. **Dumitru Baleanu:** Supervision, Funding acquisition, Writing – review & editing. **Imran Siddique:** Methodology, Writing – original draft, All authors have read and agreed to the published version of the manuscript.

Declaration of competing interest

The authors declare that they have no known competing financial interests or personal relationships that could have appeared to influence the work reported in this paper.

Acknowledgments

The author Rifaqat Ali would like to express his gratitude to Deanship of Scientific Research at King Khalid University, Saudi Arabia, for funding research groups under the research grant number G.R.P/343/42.

References

[1] A.C. Eringen, Theory of micropolar fluids, J. Math. Mech. (1966) 1–18.
[2] A.C. Eringen, Theory of thermomicrofluids, J. Math. Anal. Appl. 38 (2) (1972) 480–496.
[3] M. Waqas, M. Farooq, M.I. Khan, A. Alsaedi, T. Hayat, T. Yasmeen, Magnetohydrodynamic (mhd) mixed convection flow of micropolar liquid due to nonlinear stretched sheet with convective condition, Int. J. Heat Mass Tran. 102 (2016) 766–772.
[4] L. Ali, X. Liu, B. Ali, S. Mujeed, S. Abdal, S.A. Khan, Analysis of magnetic properties of nano-particles due to a magnetic dipole in micropolar fluid flow over a stretching sheet, Coatings 10 (2) (2020) 170.
[5] S. Abdal, B. Ali, S. Younas, L. Ali, A. Mariam, Thermo-diffusion and multislip effects on mhd mixed convection unsteady flow of micropolar nanofluid over a shrinking/stretching sheet with radiation in the presence of heat source, Symmetry 12 (1) (2020) 49.
[6] L. Ali, X. Liu, B. Ali, S. Mujeed, S. Abdal, A. Mutahir, The impact of nanoparticles due to applied magnetic dipole in micropolar fluid flow using the finite element method, Symmetry 12 (4) (2020) 520.
[7] H.M. Ali, Recent advancements in pv cooling and efficiency enhancement integrating phase change materials based systems–a comprehensive review, Sol. Energy 197 (2020) 163–198.
[8] A. Ejaz, H. Babar, H. M. Ali, F. Jamil, M. M. Janjua, I. R. Fattah, Z. Said, C. Li, Sustainable Energy Technologies and Assessments.
[9] M.A. Akram, S. Khushnood, S.L. Tariq, L.A. Nizam, H.M. Ali, The effect of grid generated turbulence on the fluidelastic instability response in parallel triangular tube array, Ann. Nucl. Energy 158 (2021) 108245.
[10] M. Khader, R.P. Sharma, Evaluating the unsteady mhd micropolar fluid flow past stretching/shirking sheet with heat source and thermal radiation: implementing fourth order predictor–corrector fdm, Math. Comput. Simulat. 181 (2021) 333–350.
[11] I. Tlili, M. Ramzan, H.U. Nisa, M. Shutaywi, Z. Shah, P. Kumam, Onset of gyrotactic microorganisms in mhd micropolar nanofluid flow with partial slip and double stratification, J. King Saud Univ. Sci. 32 (6) (2020) 2741–2751.

[12] B. Huang, L. Liu, L. Zhang, Global dynamics of 3-d compressible micropolar fluids with vacuum and large oscillations, J. Math. Fluid Mech. 23 (1) (2021) 1–50.
[13] S.U. Choi, J.A. Eastman, Enhancing thermal conductivity of fluids with nanoparticles, in: Tech. Rep., Argonne National Lab., IL (United States), 1995.
[14] J. Buongiorno, Convective Transport in Nanofluids.
[15] M. Ahmad, T. Muhammad, I. Ahmad, S. Aly, Time-dependent 3d flow of viscoelastic nanofluid over an unsteady stretching surface, Phys. Stat. Mech. Appl. (2020) 124004.
[16] A. Alblawi, M.Y. Malik, S. Nadeem, N. Abbas, Buongiorno's nanofluid model over a curved exponentially stretching surface, Processes 7 (10) (2019) 665.
[17] T. Hayat, A. Aziz, T. Muhammad, A. Alsaedi, Active and passive controls of 3d nanofluid flow by a convectively heated nonlinear stretching surface, Phys. Scripta 94 (8) (2019), 085704.
[18] S. Abdal, S. Hussain, I. Siddique, A. Ahmadian, M. Ferrara, On solution existence of mhd casson nanofluid transportation across an extending cylinder through porous media and evaluation of priori bounds, Sci. Rep. 11 (1) (2021) 1–16.
[19] B. Ali, S. Hussain, S. Abdal, M.M. Mehdi, Impact of stefan blowing on thermal radiation and cattaneo–christov characteristics for nanofluid flow containing microorganisms with ablation/accretion of leading edge: fem approach, Eur. Phys. J. Plus 135 (10) (2020) 1–18.
[20] F. Hussain, S. Abdal, Z. Abbas, N. Hussain, M. Adnan, B. Ali, R.M. Zulqarnain, L. Ali, S. Younas, Buoyancy effect on mhd slip flow and heat transfer of a nanofluid flow over a vertical porous plate, Sci. Inq. Rev. 4 (1) (2020), 01–16.
[21] B. Ali, R.A. Naqvi, Y. Nie, S.A. Khan, M.T. Sadiq, A.U. Rehman, S. Abdal, Variable viscosity effects on unsteady mhd an axisymmetric nanofluid flow over a stretching surface with thermo-diffusion: fem approach, Symmetry 12 (2) (2020) 234.
[22] Z. Abbas, S. Abdal, N. Hussain, F. Hussain, M. Adnan, B. Ali, R.M. Zulqarnain, L. Ali, S. Younas, Mhd boundary layer flow and heat transfer of nanofluid over a vertical stretching sheet in the presence of a heat source, Sci. Inq. Rev. 3 (4) (2019) 60–73.
[23] L. Ali, X. Liu, B. Ali, S. Mujeed, S. Abdal, Finite element analysis of thermo-diffusion and multi-slip effects on mhd unsteady flow of casson nano-fluid over a shrinking/stretching sheet with radiation and heat source, Appl. Sci. 9 (23) (2019) 5217.
[24] J.H. Lim, X. Zhang, G.H.A. Ting, Q.-C. Pham, Stress-cognizant 3d printing of free-form concrete structures, J. Build. Eng. 39 (2021) 102221.
[25] B. Ali, R.A. Naqvi, L. Ali, S. Abdal, S. Hussain, A comparative description on time-dependent rotating magnetic transport of a water base liquid h2o with hybrid nano-materials al2o3-cu and al2o3-tio2 over an extending sheet using buongiorno model: finite element approach, Chin. J. Phys. 70 (2021) 125–139.
[26] B. Ali, Y. Nie, S. Hussain, D. Habib, S. Abdal, Insight into the dynamics of fluid conveying tiny particles over a rotating surface subject to cattaneo–christov heat transfer, coriolis force, and arrhenius activation energy, Comput. Math. Appl. 93 (2021) 130–143.
[27] S. Arif, J. Taweekun, H.M. Ali, D. Yanjun, A. Ahmed, Feasibility study and economic analysis of grid connected solar powered net zero energy building (nzeb) of shopping mall for two different climates of Pakistan and Thailand, Case Stud. Therm. Eng. 26 (2021) 101049.
[28] B. Ali, L. Ali, S. Abdal, M.I. Asjad, Significance of brownian motion and thermophoresis influence on dynamics of reiner-rivlin fluid over a disk with non-fourier heat flux theory and gyrotactic microorganisms: a numerical approach, Phys. Scripta 96 (9) (2021), 094001.
[29] A. Kuznetsov, A. Avramenko, Effect of small particles on this stability of bioconvection in a suspension of gyrotactic microorganisms in a layer of finite depth, Int. Commun. Heat Mass Tran. 31 (1) (2004) 1–10.
[30] M.A. Bees, Advances in bioconvection, Annu. Rev. Fluid Mech. 52 (2020) 449–476.
[31] M. Khan, M. Irfan, W. Khan, M. Sajid, Consequence of convective conditions for flow of oldroyd-b nanofluid by a stretching cylinder, J. Braz. Soc. Mech. Sci. Eng. 41 (3) (2019) 116.
[32] S.U. Khan, A. Rauf, S.A. Shehzad, Z. Abbas, T. Javed, Study of bioconvection flow in oldroyd-b nanofluid with motile organisms and effective Prandtl approach, Phys. Stat. Mech. Appl. 527 (2019) 121179.
[33] K. Vajravelu, Viscous flow over a nonlinearly stretching sheet, Appl. Math. Comput. 124 (3) (2001) 281–288.
[34] R. Cortell, Viscous flow and heat transfer over a nonlinearly stretching sheet, Appl. Math. Comput. 184 (2) (2007) 864–873.
[35] S. Mukhopadhyay, Analysis of boundary layer flow over a porous nonlinearly stretching sheet with partial slip at the boundary, Alexandria Eng. J. 52 (4) (2013) 563–569.
[36] U. Sajjad, A. Sadeghianjahromi, H.M. Ali, C.-C. Wang, Enhanced pool boiling of dielectric and highly wetting liquids-a review on surface engineering, Appl. Therm. Eng. (2021) 117074.
[37] S.M. Parsa, A. Yazdani, H. Dhahad, W.H. Alawee, S. Hesabi, F. Norozpour, D. Javadi, H.M. Ali, M. Afrand, Effect of ag, au, tio2 metallic/metal oxide nanoparticles in double-slope solar stills via thermodynamic and environmental analysis, J. Clean. Prod. (2021) 127689.
[38] A. Khechekhouche, A.M. Manokar, R. Sathyamurthy, F.A. Essa, M. Sadeghzadeh, A. Issakhov, Energy, exergy analysis, and optimizations of collector cover thickness of a solar still in el oued climate, Algeria, Int. J. Photoenergy 2021 (2021) 8, 6668325.
[39] B. Gireesha, M. Umeshaiah, B. Prasannakumara, N. Shashikumar, M. Archana, Impact of nonlinear thermal radiation on magnetohydrodynamic three dimensional boundary layer flow of jeffrey nanofluid over a nonlinearly permeable stretching sheet, Phys. Stat. Mech. Appl. (2020) 124051.
[40] T. Hayat, R. Riaz, A. Aziz, A. Alsaedi, Influence of arrhenius activation energy in mhd flow of third grade nanofluid over a nonlinear stretching surface with convective heat and mass conditions, Phys. Stat. Mech. Appl. (2020) 124006.
[41] S. Abdal, H. Alhumade, I. Siddique, M.M. Alam, I. Ahmad, S. Hussain, Radiation and multiple slip effects on magnetohydrodynamic bioconvection flow of micropolar based nanofluid over a stretching surface, Appl. Sci. 11 (11) (2021) 5136.
[42] J. Singh, U. Mahabaleshwar, G. Bognár, Mass transpiration in nonlinear mhd flow due to porous stretching sheet, Sci. Rep. 9 (1) (2019) 1–15.
[43] D. Gupta, L. Kumar, O.A. Bég, B. Singh, Finite element analysis of mhd flow of micropolar fluid over a shrinking sheet with a convective surface boundary condition, J. Eng. Thermophys. 27 (2) (2018) 202–220.